Journal of
Micro/Nanolithography,
MEMS, and MOEMS

Nanolithography.SPIEDigitalLibrary.org

Digital mirror devices and liquid crystal displays in maskless lithography for fabrication of polymer-based holographic structures

Maik Rahlves
Christian Kelb
Maher Rezem
Sebastian Schlangen
Kristian Boroz
Dina Gödeke
Maximilian Ihme
Bernhard Roth

SPIE.

Digital mirror devices and liquid crystal displays in maskless lithography for fabrication of polymer-based holographic structures

Maik Rahlves,* Christian Kelb, Maher Rezem, Sebastian Schlangen, Kristian Boroz, Dina Gödeke, Maximilian Ihme, and Bernhard Roth
Leibniz Universität Hannover, Hannover Centre for Optical Technologies, Nienburger Strasse 17, Hannover D-30167, Germany

Abstract. Polymer-based holographic and diffractive optical elements have gained increasing interest due to their potential to be used in a broad range of applications, such as illumination technology, micro-optics, and holography. We present a production process to fabricate polymer-based diffractive optical elements and holograms. The process is based on maskless lithography, which is used to fabricate optical elements in photoresist. We discuss several lab-level lithography setups based on digital mirror devices and liquid crystal devices with respect to illumination efficiency, resolution, and contrast. The entire optical setup is designed with emphasis on low-cost components, which can be easily implemented in an optical research lab. In a first step, a copy of the microstructures is replicated into optical polymeric materials by means of a soft stamp hot embossing process. The soft stamp is made from polydimethylsiloxan, which is coated onto the microstructure in the photoresist. The hot embossing process is carried out by a self-made and low-cost hot embossing machine. We present confocal topography measurements to quantify the replication accuracy of the process and demonstrate diffractive optical elements and holographic structures, which were fabricated using the process presented. [DOI: 10.1117/1.JMM.14.4.041302]

Keywords: holography; diffractive optics; maskless lithography; polymer optics; spatial light modulators.

Paper 15051SSP received Apr. 15, 2015; accepted for publication Jun. 16, 2015; published online Jul. 25, 2015.

1 Introduction

Diffractive optical elements (DOE) and holographic structures lend themselves for a large variety of applications ranging from simple beam shaping to complex three-dimensional (3-D) displays.[1,2] Especially for applications in the visible range of the light spectrum as in the case of product safety items or when high diffraction angles and efficiencies are required, feature sizes of the diffractive or holographic microstructures must be decreased down to the submicron range. Hence, suitable fabrication techniques are necessary among which electron beam writing is one of the most frequently used.[2] Common fabrication processes which are capable of creating structures in the nanometer range often suffer from high process times of up to several hours and, in addition, the initial costs of these systems exceed common budgets of small research facilities or companies. Several attempts have been made to overcome these drawbacks. Especially if transmission holograms are required, polymer as material offers advantages compared to glass or silicon in terms of production costs and effort.[3,4] For small series and research purposes, laser direct writing was introduced where a focused beam is used to polymerize a monomer.[5,6] Since this technique is restricted to the optical resolution limit, two-photon polymerization was developed, which also relies on a highly focused beam but uses a nonlinear optical process in a monomer to create structures in the nanometer range below the Rayleigh diffraction limit.[7] However, both techniques are single-point processes only, which require a scanning step to generate large-area structures. Therefore, spatial light modulators (SLM) were integrated in the optical path of such devices to obtain a multifocal writing process or to be able to generate arbitrary light fields for 3-D lithography.[8,9] For smaller series or even mass production of polymer holograms or DOEs, replication techniques, such as hot embossing or injection molding, are available and allow for cost-effective copying of a metal or semiconductor mold into various polymers, such as polymethylmethacrylate (PMMA) or polycarbonate (PC). While both techniques are able to create large structures of several square centimeters at feature sizes down to a few tens of nanometers, a high precision mold is still required. For hot embossing, mold fabrication is often done by lithography which, in general, includes a lithographic mask that is placed at a few micron distance to a wafer coated with a photosensitive resist during exposure.[2,4] To achieve smaller feature sizes of well below 5 μm compared to the previous method, the mask is also projected onto the resist using imaging optics. However, using lithography masks is not only expensive but also provides only little flexibility regarding the structurable micropattern since every single holographic or DOE structure requires its own mask.

In this work, we demonstrate two different lithographic approaches, which utilize SLM instead of lithographic masks. Similar setups were reported previously for microelectromechanical systems.[10] As SLM, either digital mirror devices (DMD)[11–13] or liquid crystal displays (LCD) are

*Address all correspondence to: Maik Rahlves, E-mail: maik.rahlves@hot.uni-hannover.de

1932-5150/2015/$25.00 © 2015 SPIE

used.[14] In our work, we compare maskless lithography setups, where a DMD deflects light and generates an intensity distribution and an LCD, which changes the state of polarization of the incident light in oder to generate an intensity pattern. Both concepts can also be found in commercially available beamer systems such that both allow for potentially low-cost lithography setups. Furthermore, we introduce a complete process chain to create a hot embossing mold of a holographic or diffractive structure in a photosensitive resist. Since a photoresist is not suitable for hot embossing due to its sensitivity to thermal loads, we fabricate a negative copy of the structure in polydimethylsiloxane (PDMS), which provides suitable stress and heat resistance. The PDMS copy is subsequently used in a commercial as well as a low-cost hot embossing machine to obtain a holographic structure in PMMA. Note that our process is limited to phase modulating structures only. To obtain amplitude holograms, materials are required, which allow a local modification of their absorption properties. Such a manipulation is not possible using the method presented in this work. Furthermore, the process is capable of creating surface relief structures rather than volume holographic structures.

2 Experimental Setup

2.1 *Maskless Lithography Setup Based on a DMD*

The lithography setup based on a DMD is illustrated in Fig. 1. The DMD (Vialux ALP 4.1) consists of an array of 1024×768 single micromirrors with a pixel pitch of 13.5 μm, which deflect incoming light into two different directions. Each pixel can be addressed separately to generate an image of the microstructure to be produced. As light source, we utilize a high-power light emitting diode (LED) with a center wavelength of 435 nm and a maximum optical output power of 350 mW. To obtain a homogeneous intensity distribution on the DMD as well as a collimated beam, the emitted light from the LED is collected and collimated by a biconvex lens with a focal length of 25 mm and a flat top diffusor with an aperture angle of 20 deg (Thorlabs). The image is demagnified by a microscope setup, which consists of a tube lens (Carl Zeiss type 425308) and a plan-apochromat (Carl Zeiss Epiplan 10×) and projected onto a silicon substrate coated with photoresist (Shipley S1813). We observed that the DMD generates additional diffraction orders due to the pixel pitch of the micromirrors, which appear as multiple images between DMD and tube lens. These diffraction orders were not blocked in the setup. If higher diffraction orders contribute to image formation, a single pixel is resolved by the setup, which can be explained according to Abbe's theory of imaging. If the setup is well-aligned, higher diffraction orders do not lead to multiple or blurred images on the wafer and can be neglected. Additionally, the substrate is placed on a piezoelectric translation stage (Smaract), which can move the substrate laterally with respect to the microscope and enables us to perform a stitching process to obtain a larger structurable field size compared to the field of view of the microscope setup. When using the objective with a numerical aperture (NA) of 0.3, we obtain a field-of-view and hence a structurable area using a single exposure of 1.38×1.04 mm^2. The total structurable area depends on the travel range of the stage, which is 5 cm × 5 cm corresponding to 35×50 single exposures when using the Zeiss objective. Due to an internal positioning sensor, the stage's bidirectional positioning accuracy is >50 nm (data provided by the manufacturer), which also determines the accuracy of the stitching process. To minimize the stitching error, we generated test patterns and carried out several exposures. For each exposure run, 2×2 test patterns were stitched together. By varying the stitching offset in x and y directions, we achieved a remaining stitching error of 300 nm. However, the number of single images, which are required to fabricate structures of up to several square centimeters, may be reduced by using high-definition DMDs with a larger diagonal size at a higher resolution. To generate a sharp image of the DMD on the silicon substrate, the image reflected by the silicon wafer is imaged onto a CCD camera (Stemmer Imaging Pike F421). By manually shifting the substrate along the optical axis of the microscope lens using a mechanical translation stage (Thorlabs), we found the vertical position of the substrate where a sharp image is generated.

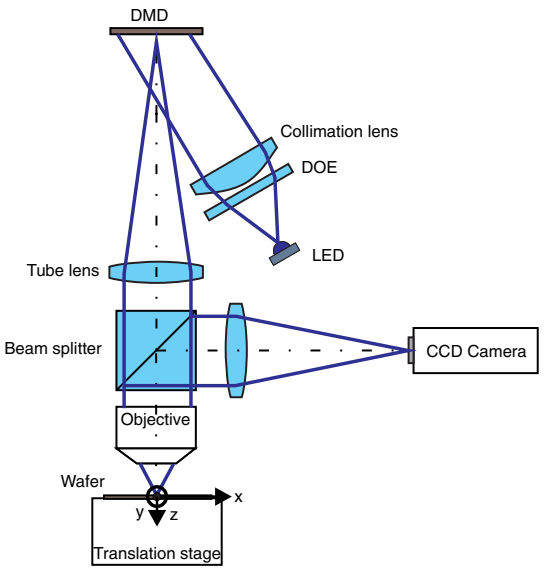

Fig. 1 Experimental setup of the maskless lithography unit using a digital mirror device (DMD).

2.2 *Maskless Lithography Setup Based on an LCD*

An alternative setup to generate an image of the master stamp geometry is based on an LCD display and is shown in Fig. 2. The basic components such as microscope translation stages and light source are equivalent to the DMD-based setup from Fig. 1. However, for image formation, the collimated light beam of the LED is polarized by a polarizing beam splitter and directed onto the LCD display (Holoeye). The LCD display consists of 1980×1024 single pixels, which rotate the polarization state of the incoming light. A mirror inside the display reflects the light back into the microscope setup passing through the polarization beam splitter again. As a consequence, the intensity of each pixel changes depending on the polarization state of the light and hence a tailored intensity distribution is generated.

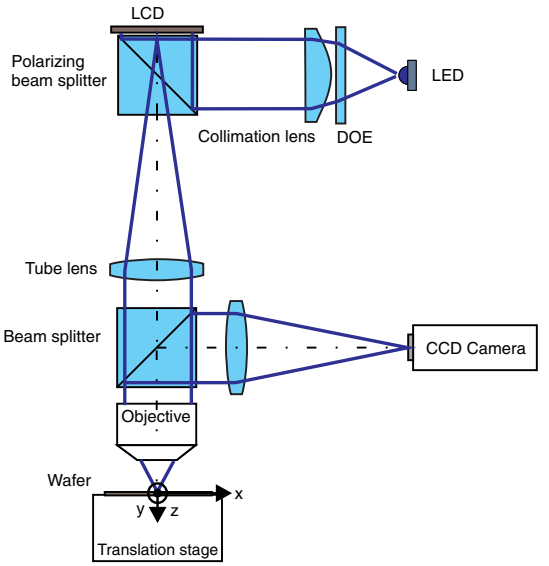

Fig. 2 Experimental setup of the maskless lithography unit using a liquid crystal display (LCD).

2.3 *Light Sources and Collimating Optics*

The most challenging aspects of a lithographic setup are a suitable choice of the light source and an adequate homogenization and collimation optics.[12] For our experiments, we chose a laser diode (Spectra-Physics Excelsior 473-50-CDRH) and a high-power LED (Roithner Lasertechnik H2A1-H435) as light sources. The technical details of the light sources used are given in Table 1. An important requirement, common to both setups described in Secs. 2.1 and 2.2, is a homogeneous illumination of the LCD and DMD. A nonuniform intensity distribution will lead to a nonuniform development rate of the photosensitive resist.

2.3.1 *Laser light source*

Lasers, compared to incoherent light sources, have the advantage that they can be easily collimated and flat top shaped intensity distributions are achievable by means of commercially available diffusers (Thorlabs). One remaining issue is speckle noise, which can be significantly reduced by rotating diffusors.[15] Since the emphasis of our work lies on low-cost setups, we did not include such devices. Furthermore, we run the setup in an ordinary lab and not under cleanroom conditions as most other lithographic systems do. Therefore, we experienced significant speckle noise due to small dust particles and, in addition, small cover glasses of the LCD and other plane parallel optical elements, such as polarizing beam splitters generate interference fringes, which are observable in every microstructure manufactured using the setup.

2.3.2 *LED light source*

In order to reduce speckle noise and interference artifacts, we also integrated a high-power LED illumination unit into the setup. A significant advantage of LED compared to lasers is that no mechanical shutter is needed to obtain a fixed exposure time during the lithographic process. To control the exposure time in case of LEDs illumination, we used a power source with a constant current and an ARDUINO microcontroller board, where the exposure can be initiated by a PC. On the other hand, light collimation and homogenization is much more difficult. We investigated several setups for this purpose: simple commercially available beam shapers for LED (Roithner Lasertechnik, Austria), a homogenization rod with a hexagonal cross section (Edmund Optics), and also flat top diffusors and collimation lenses (Thorlabs). The latter configuration showed best results in terms of a homogeneous light distribution across the SLM. Also, when comparing the DMD and LCD setups, we experienced that the DMD is more prone to collimation errors, which lead to a blurred image in the wafer plane and therefore to a significantly reduced optical resolution of the setup. Improved lithography results were obtained when the light source is placed ~50 cm away from the DMD in order to achieve better collimation. Naturally, the intensity contributing to an exposure step drops significantly when moving the light source away from the DMD. This disadvantage of DMDs is easily compensated using higher power because the damage threshold is significantly larger compared to that of LCDs. The LCD utilized in our setup has a threshold of smaller than 1 W/cm^2 and a DMD of several W/cm^2 at a wavelength of 532 nm (data provided by the manufacturer). In addition, light absorption of commonly available LCDs increases toward the ultraviolet part of the light spectrum. As a consequence, typical mercury vapor lamp emission lines at 405 nm (h-line) and 365 nm (i-line) can only be used in DMD setups. The h- and especially the i-line are of particular interest in lithography because most resists are optimized for these wavelengths and exhibit a stronger absorption peak and therefore need less energy for exposure. Whereas there are resists that also work in the g-line regime, other resists, such as SU-8, are not sensitive to g-line exposure at all, which render DMD setups the only choice for these applications.

2.4 *Autofocus*

In addition to the improvements on the illumination configuration, we integrated an autofocus system to the DMD setup. The autofocus is based on a piezoelectric driven linear translation stage (Smaract), which shifts the microscope objective along its optical axis. The camera image is used as optical feedback. To find the best focal position, a black and white

Table 1 Light sources utilized for the lithography setups.

Light source	Wavelength (nm)	Optical power (mW)	Utilized SLM	Photoresist
Laser diode	473	50	LCD	SX-3600
High power LED	435 (g-line)	380	LCD/DMD	S-1813

Note: SLM, spatial light modulator; LCD, liquid crystal display; and DMD, digital mirror device.

image is projected by the DMD onto the wafer. The focal position is obtained by shifting the positioning system until the contrast of the recorded camera image is maximal.

3 Fabrication Process

Prior to the lithography steps, we utilized a spin-coating process to obtain a homogeneous layer of photoresist S1813 (Shipley) with a thickness of ~500 nm on a substrate. A standard 3-in. silicon wafer with a thickness of 500 μm serves as substrate material. After spin coating, a prebake at 15°C was applied for 60 s. As diffractive test structure, we chose a simple grating structure with ~3 μm pitch and a macro showing a logo of our project partner.

In the subsequent process step, shown in Fig. 3, we transferred the topography of the master stamp in PDMS, which serves as a hot embossing stamp to obtain the final DOE or hologram in polymer. First, we coated a few millimeter thin layer of PDMS on the microstructured surface of the silicon substrate and cured the PDMS for 48 h at room temperature.

As material for DOE production, we chose PMMA, which is a thermoplastic polymer often used for hot embossing. The glass transition temperature of PMMA is $T_G = 105$°C. Since the emphasis of our work lies on low-cost processes, we developed a self-made low-cost hot embossing machine, as shown in Fig. 4. The advantages of the latter device are low acquisition costs but it provides only a limited capability to control the embossing force. Our self-made hot embossing machine consists of a tool holder and a substrate holder. Both are mounted on two 200 W heating plates, whose temperature is monitored by PT100 thermistors. Each thermistor is connected to a control unit, which sets the heating level to a preset temperature value. The embossing force is applied manually using a hydrostatic pressure pump. To achieve a steady relative movement as well as to provide negligible tilt error between the tool and substrate holder, the latter is guided by guiding rods during an embossing cycle. Due to the simple setup, our lab-level embossing machine can be built for less than 2000 USD, which renders it affordable even for small research units of companies.

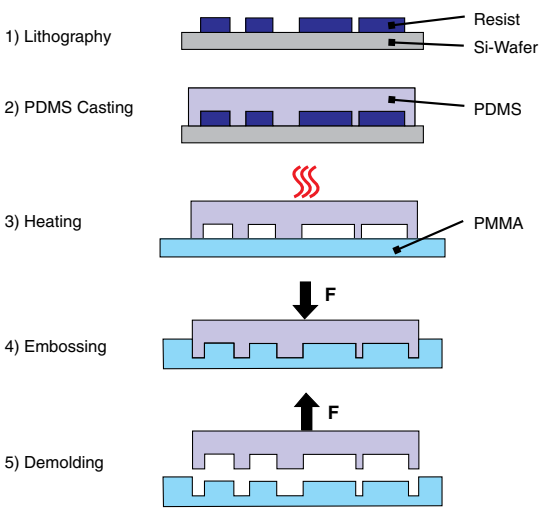

Fig. 3 Replication process for master stamp replication into polymethylmethacrylate (PMMA) using soft stamp hot embossing.

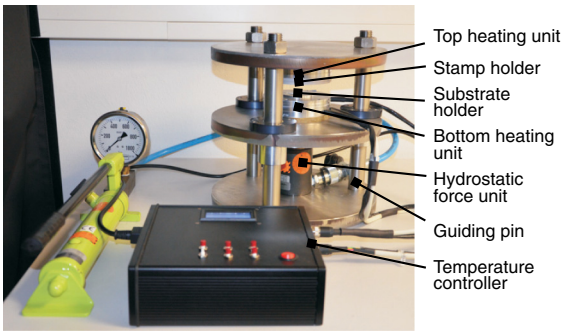

Fig. 4 Lab-level low-cost hot embossing machine.

For comparison, we conducted two embossing runs using our self-made as well as our commercial hot embossing machine HEX 03 (Jenoptik). The first run was carried out in the commercial device. Both PDMS tool and PMMA substrate of 500-μm thickness were heated to an embossing temperature of 120°C and an embossing pressure of 6.2 kPa was applied for 5 min. The PMMA DOE was removed manually from the PDMS after cooling down to an release temperature of 40°C. The second embossing run was performed in the self-made hot embossing machine, where we also used a hot embossing temperature of 120°C. However, since our device does not include a pressure sensor, the exact embossing pressure could not be determined.

4 Results and Characterization

4.1 *Master Stamp Fabrication by DMD- and LCD-Based Maskless Lithography*

Figure 5 shows microscope images of the master stamps, which were created in photoresist utilizing the DMD- and the LCD-based setups. Both structures consist of linear diffraction gratings with period lengths of 5.4 and 3 μm, respectively. However, the pattern generated using the DMD shows periodical defects at the side walls of the linear structures, which are apparent in the enlargement of the microscope image in Fig. 5. By contrast, the structures generated using an LCD show a significantly smaller line edge roughness. The roughness in the first image is due to a larger pixel size of 13.8 μm of the DMD in comparison to the LCD, which exhibits a pixel pitch of 8 μm. When using a microscope lens with NA of 0.3, the theoretical resolution of the setup is 884 nm on the wafer, which corresponds to resolved pixel of 8.8 μm in the display plane of the setup when considering a magnification of 10 of the microscope lens. Hence, the setup resolves the DMD micromirrors but not

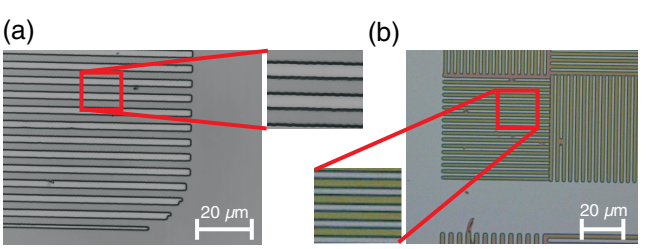

Fig. 5 Microscope images of master stamps created in photoresist using (a) the DMD-based setup and (b) the LCD-based setup.

the single-LCD elements. This effect weakens when using objectives with higher NAs. When comparing the results of both setups, we experienced that much more effort has to be made when designing suitable collimation optics for DMD compared to LCD based setups. Using an LCD, only a homogeneous light distribution must be generated to yield a uniform development of all microstructures throughout the entire field of view of the setup. For DMD illumination, it is not only necessary to consider a homogeneous light distribution, but it is also necessary that each light ray which is reflected by a micromirror is perfectly parallel to the optical axis of the microscope setup. A violation of this condition leads to a blurred image of the microstructure and hence to significant decrease in the smallest achievable feature size of the setup. On the other hand, most DMDs, in contrast to common LCDs, can be used in combination with ultraviolet light sources, which allow for a greater variety of photoresists to be used. In addition, DMDs display less light absorption and higher light intensities are feasible to reduce the exposure time. In our case, an exposure cycle for a single image was 7 min and 10 s using the LCD and DMD setups, respectively.

4.2 *Hot Embossing Results*

A photograph of the PDMS copy obtained from the master stamp fabricated using the DMD based setup as well as a hot embossed PMMA replica utilizing the commercial HEX03 machine is shown in Fig. 6(a). A DOE fabricated by our self-made hot embossing machine in PMMA is shown in Fig. 6(b). Both embossing results show a logo of our project partner as macro-geometry and a diffraction grating with 5.2 μm pitch is incorporated in addition inside the logo, which leads to light diffraction as observable in Fig. 6. We carried out confocal topography measurements to quantify the error between master stamp, PDMS soft stamp, and PMMA replica. We found that, in general, the microstructures are well replicated. The measured periods are 5.22, 5.32, and 5.37 μm and the measured profile heights are 492, 431, and 471 nm of the master stamp, the PDMS stamp, and the PMMA replica fabricated using the HEX03, respectively. The increase in period length is caused by an expansion of the PDMS and PMMA during hot embossing due to the embossing force and polymer yielding. For comparison, Fig. 7 shows 3-D confocal microscope measurements of master stamp and PMMA replica. The measured topography shows the same section on the sample as in Fig. 6.

The smallest achieved line width of the PMMA replica in Fig. 7 accounts for 1.36 μm, which corresponds to a smallest achievable period length $\Lambda = 2.72$ μm when using an objective with NA = 0.3 and a DMD. For comparison, Table 2 shows the resolution d_{res} of the lithographic setup and the corresponding period length Λ as function of the NA of the objective used for demagnification. The NA values of 0.3_{DMD} and 0.3_{LCD} relate to the DMD- and LCD-based setups used for the lithographic processes, respectively. All values in Table 2 given for NAs larger than 0.3 are theoretical values assuming a diffraction limited setup. Experiments using objectives with a NA larger than 0.3 will be included in our future work.

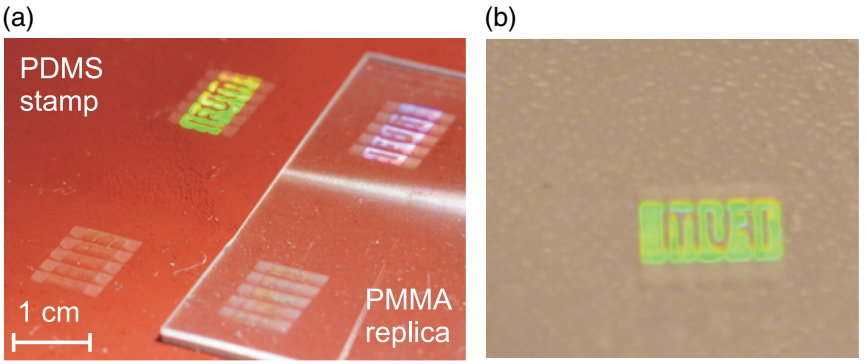

Fig. 6 Large area diffractive structure on polydimethylsiloxane stamp and corresponding PMMA replica fabricated using (a) the HEX03 and (b) the self-made hot embossing machine.

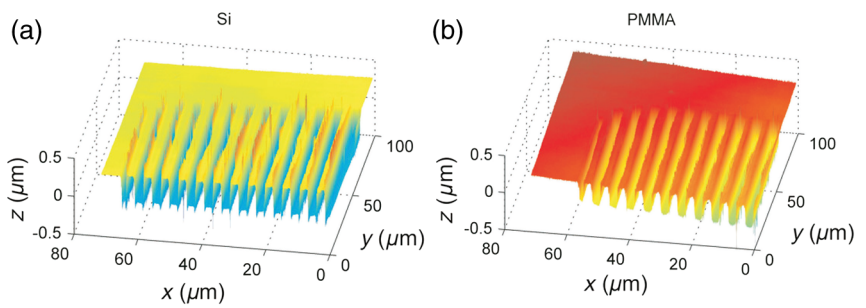

Fig. 7 Confocal topography measurements: (a) a stamp in photoresist on silicon substrate and (b) a PMMA replica.

Table 2 Influence of numerical aperture (NA) of the lithographic objective on the optical resolution d_{res}, the grating period length Λ, and angle between zeroth and first diffraction order θ_{diff} at a wavelength of 633 nm; theoretical values are indicated by *.

NA	d^*_{res} (nm)	Λ (nm)	θ^*_{diff} (deg)
0.3_{DMD}	824	2723	11.27
0.3_{LCD}	824	1623	19.13
0.5^*	494	988	32.58
0.7^*	353	706	48.90
0.9^*	275	550	75.30
$1.4^{*,immersion}$	176	352	—

4.3 *Optical Characterization of the PMMA Replica*

Optical properties of gratings and holographic structures depend, in general, on profile height and period length Λ as well as on transmission and reflection coefficients of the material utilized as substrate material for the hot embossing process. In addition to the period length and profile height, we also determined the diffraction efficiency η for the PMMA grating in transmission and reflection. The PMMA sample, shown in Fig. 6, was illuminated by a He-Ne laser beam with a center wavelength of 633 nm. The sample was aligned such that the laser beam only illuminates the grating region. We measured the total power $P_{tot} = 73.0\ \mu W$ of the laser beam before passing the sample and the total power $P_{trans} = 66.4\ \mu W$ of the transmitted light by placing a power measuring device (Thorlabs S121C) directly behind the sample. The power loss, $P_{trans} - P_{tot}$, is readily explained by the Fresnel reflex at the air–PMMA interfaces of the sample and hence, absorption inside the sample can be neglected due to the small sample thickness of $\sim 500\ \mu m$. The diffraction efficiency η_{trans} of the transmitted light was determined by measuring the power $P = 15.8\ \mu W$, which was diffracted into the first order and yields $\eta_{trans} = 0.24$. The reflected diffraction efficiency $\eta_{refl} = 0.19$ was estimated from the measured power $P_{refl} = 0.59\ \mu W$ of the light, which was reflected into the first diffraction order and the Fresnel reflex of $3.04\ \mu W$, which was calculated from P_{total} assuming a refractive index of PMMA of 1.49.[3] For PMMA, we may assume the same transmission and reflectance properties in the entire visible range of the spectrum.[3]

5 Conclusion

We presented two different optical setups for maskless lithography based on a DMD and an LCD, respectively. Our experimental results show that even if the optical setup and especially the optical design of the light source is less complicated using the LCD, the setup utilizing a DMD provides advantages regarding process time and operation at a shorter wavelength. Using maskless lithography, we introduce a process chain for low-cost production and replication of polymer-based diffractive optical elements and holographic structures. The process chain relies on an initial lithographic process step, where a master is fabricated by means of maskless lithography. In a subsequent step, we transferred the micro- and macrogeometry of the fabricated master stamp into a PDMS copy, which was used for soft stamp hot embossing. We also presented hot embossing results of diffractive structures obtained by using a self-made and low-cost hot embossing machine. The casting quality of the results was compared to embossing results obtained by using a professional hot embossing machine. No significant deviation in quality was observed. Hence, the presented process chain enables us to fabricate diffractive optical elements at high optical quality on a low-cost and lab-level basis. In the future, our results will also be used to fabricate more-complex optical structures, such as optical waveguide structures, arrayed waveguide gratings, microresonators, and resonant or interferometric sensors.

Acknowledgments

A part of this work was funded by the German Research Foundation (DFG) in the framework of the Collaborative Research Center PlanOS and the German Federation of Industrial Research Associations (AiF) under Grant No. EFB ZN 500.

References

1. S. Sinzinger and J. Jahns, *Micro-Optics*, Wiley-VCH, Weinheim (2003).
2. H. Herzig, Ed., *Micro-Optics—Elements, Systems and Applications*, Taylor & Francis, London, UK (1997).
3. S. Bäumer, Ed., *Handbook of Plastic Optics*, Wiley-VCH, Weinheim (2005).
4. M. Worgull, *Hot Embossing: Theory and Technology of Microreplication*, William Andrew, Oxford, UK (2009).
5. Y.-C. Chan et al., "Development and applications of a laser writing lithography system for maskless patterning," *Opt. Eng.* **37**(9), 2521–2530 (1998).
6. M. T. Gale et al., "Fabrication of continuous-relief micro-optical elements by direct laser writing in photoresists," *Opt. Eng.* **33**(11), 3556–3566 (1994).
7. J. Serbin et al., "Femtosecond laser-induced two-photon polymerization of inorganic–organic hybrid materials for applications in photonics," *Opt. Lett.* **28**(5), 301–303 (2003).
8. G. Vizsnyiczai, L. Kelemen, and P. Ormos, "Holographic multi-focus 3D two-photon polymerization with real-time calculated holograms," *Opt. Express* **22**(20), 24217–24223 (2014).
9. N. J. Jenness et al., "A versatile diffractive maskless lithography for single-shot and serial microfabrication," *Opt. Express* **18**(11), 11754–11762 (2010).
10. J. Lake et al., "Maskless grayscale lithography using a positive-tone photodefinable polyimide for MEMS applications," *J. Microelectromech. Syst.* **20**(6), 1483–1488 (2011).
11. M. Rahlves et al., "A flexible, fast, and low-cost production process for polymer based diffractive optics," *Opt. Express* **23**(3), 3614–3622 (2015).
12. C. Liu et al., "Imaging simulation of maskless lithography using a DMD," *Proc. SPIE* **5645**, 307–314 (2005).
13. L. H. Erdmann et al., "MEMS-based lithography for the fabrication of micro-optical components," *Proc. SPIE* **5347**, 79–84 (2004).
14. B.-A. Behrens et al., "Method to emboss holograms into the surface of sheet metals," *Key Eng. Mater.* **549**, 125–132 (2013).
15. J. C. Dainty, Ed., *Laser Speckle and Related Phenomena*, Springer, Berlin (1975).

Maik Rahlves received his diploma in physics in 2006 and his PhD in mechanical engineering in 2011 from the Carl-von-Ossietzky University and Leibniz University Hannover, respectively. Since 2009, he has been with the Hanover Center for Optical Technologies, Leibniz University Hanover, where he has headed the applied optics group since 2011. His research interests are optical metrology, holography, and polymer-based micro-optics.

Christian Kelb received his diploma degree in mechanical engineering in 2011 from the Leibniz University Hanover. He is currently pursuing his PhD degree in engineering at the Hanover Center for Optical Technologies (HOT) of the Leibniz University Hanover. He is currently working in the field of optical technologies, in particular,

optical sensing and manufacturing by means of lamination, hot embossing, and injection molding.

Maher Rezem received his diploma degree in electrical engineering in 2012 from the Karlsruhe Institute of Technology. He is currently pursuing his PhD degree in engineering at the Hanover Center for Optical Technologies (HOT) of the Leibniz University Hannover. He is currently working in the field of polymer optics manufacturing by means of hot embossing and UV-imprinting.

Sebastian Schlangen received a BS degree in biomedical engineering from the University of Applied Science Aachen in 2012. He obtained his MS degree in biomedical engineering in 2014 at the Leibniz University Hannover, where his work was focused on medical imaging and laser applications in medical technology. Since June 2014, he has been a PhD candidate at the Hanover Center for Optical Technologies. His research interests include digital and computer-generated holography.

Kristian Boroz is a student assistant at the Leibniz Universität Hannover.

Dina Gödeke is a graduate student at the Leibniz Universität Hannover. Her major is mechanical engineering.

Maximilian Ihme is a mechnical engineering student at the Leibniz Universität Hannover. He is currently working on his MS thesis.

Bernhard Roth graduated from the University Bielefeld (PhD) in atomic physics in 2001. From 2002 to 2007, he was group leader at the University Duesseldorf, where he obtained his state doctorate (Habilitation) in quantum optics. Since 2012, he has been director of the Hannover Center for Optical Technologies (HOT) and professor of physics at the Leibniz University Hannover. His activities include laser development and spectroscopy, polymer optical sensing, as well as biomedical optics and imaging.